Chloride Permeability and Microstructure of Portland Cement Mortars Incorporating Nanomaterials

Xiaodong He and Xianming Shi

Chloride permeability of concrete has been recognized as a critical intrinsic property affecting the durability of reinforced concrete. An experimental study was done, designed to examine the chloride permeability and microstructure of portland cement mortar with nanomaterials admixed at 1% by weight of cement. The electromigration test showed that, for cement mortars of the same mix design, the incorporation of nanoparticles (Fe_2 O_3, Al_2O_3, TiO_2, and SiO_2) and nanoclays (montmorillonite) improved the chloride penetration resistance of the mortar, as indicated by the reduced apparent diffusion coefficients of chloride anion. The nanomaterials also reduced the general ionic permeability of the mortar, as indicated by the reduced electric charge passing through. Such improvements were especially significant when using nano-SiO_2 and nanoclays. The electrochemical impedance spectroscopy test indicated that incorporation of nanomaterials in cement mortar significantly increased its ionic transport resistance and decreased its electric capacitance, and again such effects were especially significant when using nano-SiO_2 and nanoclays. The field emission scanning electron microscopy test revealed that the admixing of nanomaterials not only led to denser cement mortar but also changed the morphology of cement hydration products. Mechanisms are proposed to explain the physicochemical changes induced by the nanomaterials and the specific surface area of nanomaterials is demonstrated as one of the key factors. Considering the low cost of nanoclays, their use in concrete to reduce chloride permeability and to improve other properties of concrete is promising.

The construction industry is one of many that have identified nanotechnology as a promising emerging technology. Furthermore, ready mix concrete and concrete products were identified as among the top 40 industrial sectors likely to be influenced by nanotechnology in 10 to 15 years (*1*). Nonetheless, construction has lagged behind other industries where nanotechnology research and development (R&D) have attracted significant interest and investment from large industrial corporations and venture capitalists. Recognizing the huge potential and importance of nanotechnology to the construction industry, the European Commission in late 2002 approved funding for the Growth Project GMA1-2002-72160 NANOCONEX, toward setting up a network of excellence in nanotechnology in construction. In the United States, the research on nanotechnology-based concrete materials is still burgeoning.

Despite their undisputed importance, omnipresence, and low-technology status, cement-based materials are among the least understood materials due to their complex nature (*2*). Particularly, reinforced concrete is a composite material with features of various dimensions ranging from nanometer-sized pores and calcium-silicate-hydrate (C-S-H) gel to steel reinforcement that can be meters in length, to aggregate particles of all sizes in between. The properties of such composite material are further complicated by the time-dependent nature of the species binding and cement hydration processes that start at the mixing of cement clinker minerals with water and continue for months or even years.

Concrete, as a porous and highly heterogeneous composite, is subject to the ingress of various ionic and molecular species from the natural environment and human activities. Excessive accumulation of some species can be deleterious to the service life of concrete structures. For instance, carbonation, chloride ingress, and sulfate attack are the major environmental loadings that cause deterioration of concrete and subsequent reduction in the strength, serviceability, and aesthetics of the structure (*3*). The ingress of gases, water, or ions in aqueous solutions into concrete takes place through pore spaces in the cement paste matrix and paste-aggregate interfaces or microcracks. For the durability of concrete, permeability is believed to be the most important characteristic (*4*), which is related to its microstructural properties, such as the size, distribution, and interconnection of pores and microcracks (*5*).

The properties of a material originate from its structure and chemical composition. However, it is still a challenge to elucidate the complex correlations between transport properties of concrete and the structure and chemistry of concrete at various scales. At the macroscopic level (visible, usually >200 µm), hydrated concrete can be viewed as a three-phase material consisting of aggregate particles of varying sizes and shapes, an incoherent mass of the hydrated cement paste, and entrapped (as large as 3 mm) or entrained (usually 50 to 200 µm) air voids in the hydration products. The type, amount, and distribution of these phases are critical to the transport properties of concrete (*6*). An examination at the micron scale distinguishes a fourth phase, that is, interfacial transition zone (ITZ) that represents a thin-shell region (typically 10 to 50 µm thick) surrounding large aggregate particles (*7*).

BACKGROUND

In the past decade, rapid progress and improved availability of advanced nanomaterials and characterization techniques have led to a few studies examining the microstructures, properties, and

---

Corrosion and Sustainable Infrastructure Laboratory, Western Transportation Institute, Montana State University, P.O. Box 174250, Bozeman, MT 59717-4250. Corresponding author: X. Shi, Xianming_s@coe.montana.edu.

Transportation Research Record: Journal of the Transportation Research Board, No. 2070, Transportation Research Board of the National Academies, Washington, D.C., 2008, pp. 13–21.
DOI: 10.3141/2070-03

underlying mechanisms of cement-based materials with nanoparticles or nanoclays admixed. Li et al. found that both the 7-day and 28-day compressive and flexural strengths of cement mortars mixed with nano-Fe_2O_3 and nano-SiO_2 were higher than those of a plain cement mortar, and the mechanism suggested by the scanning electron microscopy (SEM) study was that the nanoparticles filled up the pores and reduced $Ca(OH)_2$ compound among the hydrates (*8*). Ji found that for concretes of similar 28-day strength, the incorporation of nano-SiO_2 enhanced the water penetration resistance of concrete, and the SEM study revealed that nano-SiO_2 also led to more uniform and compact concrete (*9*). The effect of nano-SiO_2 on concrete was attributed to its ability to react with $Ca(OH)_2$ crystals and produce C-S-H gel, and its ability to fill the voids of C-S-H gel structure. Tsai found that adding as little as 0.3% or 0.5% of nanoclay by weight of cement enhanced the compressive strength of concrete, but it failed to improve its thermoconductivity (*10*). Birgisson reported that a polymer-modified nanoclay was able to enhance both the strength and ductility of concrete and to significantly reduce its permeability and shrinkage and attributed the enhancements to the pozzolanic effect and exfoliation effect (*11*). Chang et al. found that adding 0.6% and 0.4% of nanoclay (montmorillonite in liquid form) by weight of cement achieved the optimum performance of portland cement paste nanocomposite, increasing its 28-day compressive strength by 13% and reducing its gas permeability coefficient by 50%, respectively (*12*). In addition, microstructural properties analyzed by X-ray diffraction, differential scanning calorimetry, nuclear magnetic resonance, and mercury intrusion porosimetry indicated that the microstructures of cement paste with nanomontmorillonite contained more dense solid material and more stable bonding framework (*12*).

Concrete is the most widely used manufactured building material in the world, owing to its versatility and relatively low cost. Approximately 6 billion cubic m of concrete are made each year, equal to 1 cubic m per capita on Earth. Concrete has also become the material of choice for the construction of structures exposed to extreme conditions (*13*). As such, even slight improvements in the design, production, and materials performance of concrete can have enormous social and economic impacts.

For reinforced concrete structures exposed to salt-laden environments, chloride-induced corrosion of reinforcing steel is the major cause for their premature deterioration and degradation. Chloride anions can act as a catalyst in the anodic reaction of corrosion process once they penetrate the concrete cover and reach a threshold level high enough to disrupt the passive film on rebar surface (typically a ferrous hydroxide layer of nanometers thick). Such depassivation of passive film on a rebar surface usually leads to subsequent accelerated corrosion if no protective action is taken (*14, 15*). Therefore, chloride permeability has been recognized as a critical intrinsic property of the concrete (*16*).

This study aimed to systematically evaluate the chloride permeability of portland cement mortar incorporating various nanomaterials at 1% by weight of cement. The nanomaterials investigated include nanosized particles (Fe_2O_3, Al_2O_3, TiO_2, and SiO_2) and two nanomontmorillonites (one is hydrophilic and the other is hydrophobic due to the modification by polysiloxane). Electromigration, electrochemical, and surface analytical measurements were conducted to investigate the effect of nanomaterials on the ionic transport resistance (including chloride permeability) and microstructure of portland cement mortar.

EXPERIMENTAL METHODS

Material Properties

The cement mortars used Type I portland cement. The fine aggregates used were river sand sieved to allow a maximum aggregate size of 2 mm before proportioning and admixing. Nanoparticles (Fe_2O_3, Al_2O_3, TiO_2, and SiO_2) were purchased from MTI Corporation. Nanoclays 1.44PS (Clay-ho) and PGW (Clay-hi) were obtained from Nanocor Inc. The properties of nanoparticles and nanoclays are listed in Table 1.

Specimen Fabrication

For both the control (with no nanomaterials admixed) and the nanomodified cement mortars, three specimens were fabricated to ensure the statistical reliability of chloride permeability test results. For the nanomodified ones, nanomaterials were first mixed into cement in a mixer, and then water was added and stirred at a high speed (~250 rpm) for 5 min. Afterward, sand was added into the mixture and stirred at a low speed (~60 rpm) for about 1.5 min to achieve good workability. The ratio of cement: sand: water: nanomaterial by weight was 1: 1: 0.5: 0.01. After mixing, the fresh mixture was poured into molds to form Φ 40 mm × 5 mm discs, which was carefully compacted to minimize the amount of entrapped air. The cement mortar specimens were demolded after 24 h and then cured in a wet chamber (relative humidity in excess of 95%, temperature 20°C) for 28 days, before being subjected to the electromigration test.

TABLE 1 Properties of Nanomaterials Used in Study

Nanomaterial	Bulk Density (g/cm^3)	Maximum Size (nm)	Specific Surface Area (m^2/g)
Clay-ho: 1.44PS (polysiloxane-modified montmorillonite)	0.251	200–400 (aspect ratio)	~7,968[a]
Clay-hi: PGW (98% montmorillonite)	0.678	200–400 (aspect ratio)	~2,950[a]
SiO_2	0.063	30	440
TiO_2 (anatase)	0.15–0.25	5	210
Al_2O_3 (gamma)	0.16–0.4	10	180
Fe_2O_3 (gamma)	1.20	30	30

[a] The specific surface area for the nanoclay was estimated based on bulk density, assuming a perfect sheet structure of montmorillonites with 1-nm spacing. Other data are from the suppliers.

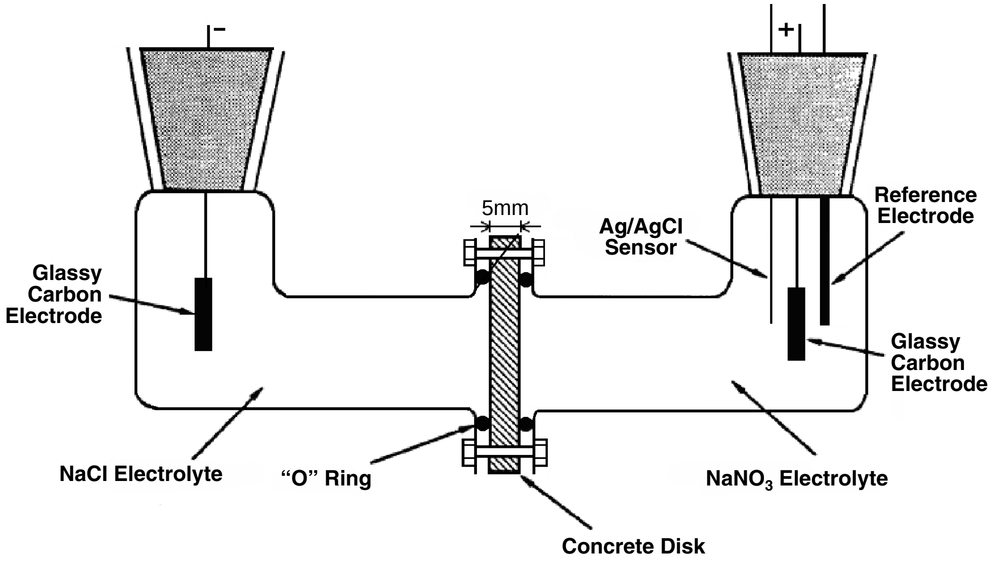

FIGURE 1 Experimental setup for electromigration tests.

Characterization

Electromigration Measurements

To test the chloride permeability of cement mortars, electromigration experiments were performed using the glass cell as shown in Figure 1. The glass cell features a disc-shaped mortar specimen that separates the chloride anion source (3% NaC1) and the destination solution (4.3% $NaNO_3$). Each of the two half-cells contains one glassy carbon electrode with an exposed surface area of 1 cm^2. Once the mortar disc, electrolytes, and electrodes were in place, a 5-V DC electric field was maintained across the disc through the two carbon electrodes in the two compartments. During the test, readings of open circuit potential (OCP) of the Ag–AgCl sensor in the destination solution were taken periodically, using a saturated calomel electrode (SCE) as the reference electrode. In addition, the current passing through the disc was monitored using a Gamry Electrochemical Multiplexer ECM8 Potentiostat. The Ag–AgCl sensor was used to monitor the evolution of free chloride anion (Cl^-) concentration in the destination solution, as their OCP data were compared against a standard calibration curve correlating potential readings with known Cl^- concentrations.

The method used to calculate the apparent diffusion coefficient *D* of Cl^- in cement mortars is described as follows. Under an externally imposed electric field with an intensity of *E*, the mobility of ions (ν, the average velocity of ions per unit of electric field) is related to the diffusion coefficient through the Nernst-Einstein equation (*17*):

$$\nu = \frac{zFD}{RT}$$

where

z = charge number,
F = Faraday constant,
R = gas constant, and
T = absolute temperature.

The chloride ion mobility can be calculated from the time t_0 required for the chloride front to penetrate a depth *d* of the specimen (*18*):

$$\nu = \frac{d}{t_0 E}$$

Therefore, the diffusion coefficient *D* of Cl^- in cement mortars can be estimated by the following equation:

$$D = \frac{dRT}{t_0 E_z F}$$

Figure 2 provides an example of how the chloride penetration time t_0 was estimated from the monitored Cl^- concentrations in the anolyte (destination solution). The t_0 is the point after which the Cl^- concentration in the anolyte increases linearly with time.

Electrochemical Measurements

At the end of each electromigration test, the Gamry Potentiostat was used to measure electrochemical impedance spectra (EIS) data, to

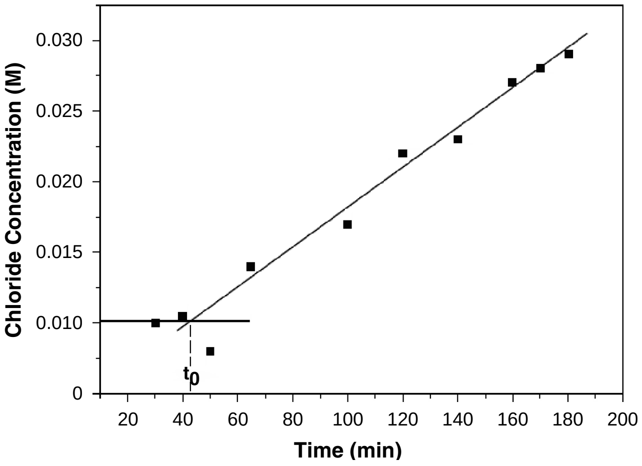

FIGURE 2 Typical evolution of chloride concentration in anolyte over time.

characterize the microstructural properties of cement mortar. To this end, a platinum mesh was placed in the left (cathodic) compartment to serve as the counter electrode, whereas the carbon electrode and the SCE in the right (anodic) compartment served as the working electrode and the reference electrode, respectively. The EIS measurements were taken by polarizing the working electrode at ±10 mV around its OCP, using sinusoidal perturbations with a frequency between 300 KHz and 5 mHz (10 points per decade). The Gamry analysis software was used to plot and fit the EIS data.

Surface Analytical Measurements

For surface analysis, the mortar specimens were taken out of the glass cell after the electromigration and electrochemical measurements. A slice sample was cut directly from the side of mortar disc exposed to the chloride anion source (3% NaC1). After being vacuum dried, the samples were then subjected to a field emission scanning electron microscope [(FESEM), Zeiss Supra 55VP] to study the localized morphologies of cement mortar at the microscopic level, using a Hitachi S-4100 system with beam energy of 25.0 keV.

DISCUSSION OF RESULTS

Effect of Nanomaterials on Ionic Permeability of Cement Mortar

The electromigration test showed that, for cement mortars of the same mix design, the incorporation of nanoparticles (Fe_2O_3, Al_2O_3, TiO_2, and SiO_2) and nanoclays (montmorillonite) improved the chloride penetration resistance of the mortar, as indicated by the reduced apparent diffusion coefficients of chloride anion, D_{Cl^-}. Such improvements were especially significant when using nano-SiO_2 and nanoclays. Figure 3 shows the apparent diffusion coefficients of Cl^- in the portland cement mortars tested, with the mean and standard deviation calculated from two or three specimens. When nano-SiO_2, hydrophilic nanomontmorillonite, and hydrophobic nanomontmorillonite were admixed into fresh cement mortar at 1% by weight of cement, the value of D_{Cl^-} was decreased by 61.7%, 66.4%, and 76.0%, from 6.82×10^{-11} m^2/s (control specimen) to 2.61×10^{-11} m^2/s, 2.29×10^{-11} m^2/s, and 1.64×10^{-11} m^2/s, respectively. The reduction of D_{Cl^-} induced by the nanomaterials was in the order of Clay-ho > Clay-hi > SiO_2 > TiO_2 > Al_2O_3 > Fe_2O_3, which is exactly the order of specific surface area (SSA) of these nanomaterials (see Table 1).

The evolution of electric current was monitored during the electromigration test and then used to calculate the amount of electric charge passing through the mortar discs by integrating the current curve over time. Results showed that, for cement mortars of the same mix design, the incorporation of nanoparticles and nanoclays reduced the general ionic permeability of the mortar, as indicated by the reduced electric charge passing through, *Q*. Again, such improvements were especially significant when using nano-SiO_2 and nanoclays. When nano-SiO_2, hydrophilic nanomontmorillonite, and hydrophobic nanomontmorillonite were admixed into fresh cement mortar at 1% by weight of cement, the value of *Q* (over 225 min) was decreased by 27.4%, 35.5%, and 54.0%, from 6.77×10^4 C/m^2 (control specimen) to 4.91×10^4 C/m^2, 4.37×10^4 C/m^2, and 3.11×10^4 C/m^2, respectively. The reduction of *Q* induced by the nanomaterials was in the order of Clay-ho > Clay-hi > SiO_2 > TiO_2 > Al_2O_3 > Fe_2O_3, which is exactly the order of SAA of these nanomaterials (see Table 1).

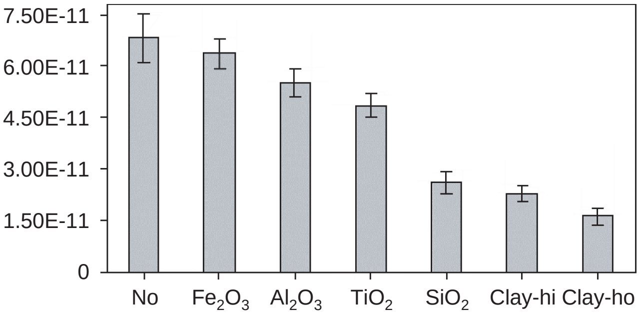

FIGURE 3 Apparent diffusion coefficient of Cl^- in cement mortars (m^2/s).

Figure 4 further illustrates the strong correlation between the SSA of nanomaterial and the chloride permeability (Figure 4*a*) as well as the general ionic permeability (Figure 4*b*). As the SAA of nanomaterials increased (from nano-Fe_2O_3, nano-Al_2O_3, and nano-TiO_2, to nano-SiO_2 and nanomontmorillonites), both D_{Cl^-} and *Q* decreased exponentially, indicating enhanced resistance to both the penetration of Cl^- and other ions into the mortar specimens. The electromigration test results revealed that the small amount of nano-SiO_2 and nanoclays markedly improved the chloride penetration resistance of the cement mortars. These findings show the promise for using nanomaterials to improve concrete durability.

Effect of Nanomaterials on Microstructure of Cement Mortar

Investigation by Electrochemical Impedance Spectroscopy

EIS provides information on interfaces and thus was used to shed light on the microstructural properties of the cement mortars used in this study. The complex impedance of the mortar–electrolyte interfaces depends on the frequency of the externally imposed alternating current polarization signal, allowing the representation of the system with an equivalent circuit typically consisting of resistors and capacitors. For this study, the equivalent circuit shown in Figure 5 was used to characterize the interfaces between the counter electrode and the working electrode separated by the mortar disc. Constant phase elements (*Q*) instead of capacitances were used in all fittings. Such modification is obligatory when the phase angle of capacitor is different from –90°.

The EIS parameters that characterize the electrolyte–concrete interface are the ionic transport resistance of the mortar disc (R_{mortar}) and the capacitance (in this case, constant phase element) of the disc (Q_{mortar}). Table 2 presents the fitted equivalent circuit parameters of both the control and nanomodified mortar discs, in which n_{mortar} is the fitting coefficient for Q_{mortar} (with 1 being the perfect fit of a capacitor and 0 being the worst).

As shown in Table 2, compared with the plain portland cement mortar disc, the discs modified by nanoparticles (Fe_2O_3, Al_2O_3, TiO_2, and SiO_2) and nanoclays (montmorillonite) had higher values of R_{mortar} and lower values of Q_{mortar}. R_{mortar} characterizes the porosity of the mortar disc and is a function of the resistance of ionic transport through the interconnected pores, cracks, and potentially air voids in the disc. The increased ionic transport resistance and decreased electric capacitance of nanomodified mortar discs suggest that the incorporation of nanomaterials led to denser microstructure of cement

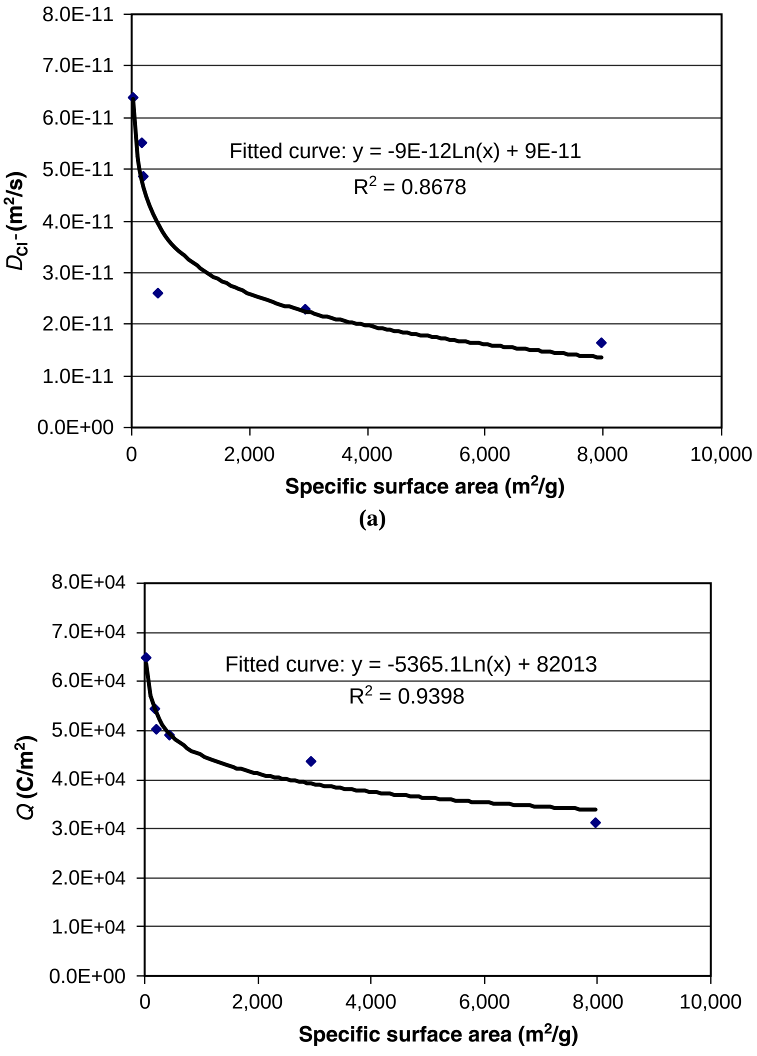

(a)

(b)

FIGURE 4 Correlation between SAA of nanomaterial and (*a*) apparent diffusion coefficient of Cl^- and (*b*) electric charge passing through cement mortars over 225 min.

mortar. Such effects were especially significant when using nano-SiO_2 and nanoclays. Compared with the plain portland cement mortar disc, the nanomodified mortar discs had higher values of n_{mortar}, possibly due to lower porosity and higher microstructural regularity of the discs.

A strong correlation was found between D_{Cl^-} and both the ionic transport resistance and the electric capacitance of portland cement mortars. As the diffusion coefficient of Cl^- in portland cement mortar decreased (from control, to nanoparticle modified mortar and nanomontmorillonite modified mortar), R_{mortar} increased exponentially, whereas Q_{mortar} decreased exponentially. These three parameters were all indicators of the microstructure and chemical composition of the saturated mortar matrix, in which the ionic species transport mainly via natural diffusion or electromigration.

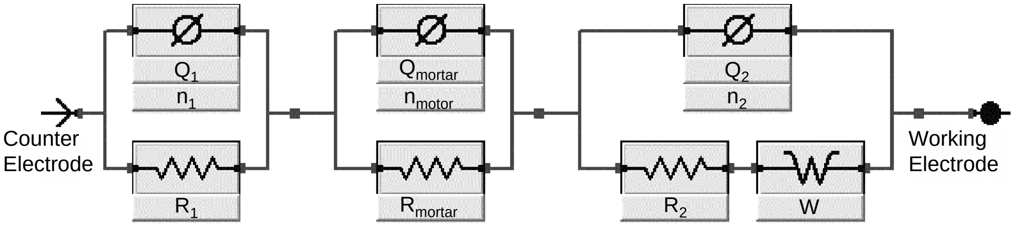

FIGURE 5 Equivalent circuit used for fitting impedance spectra.

TABLE 2 Equivalent Circuit Parameters of Mortar Discs

Mortar Specimen	R_{mortar} (KΩ cm^2)	Q_{mortar} (μS cm^{-2})	n_{mortar}
Control (without nanomaterial)	7.03±2.03	776±140	0.03±0.01
Mortar with nano-Fe_2O_3	24.05±8.57	387±35.5	0.67±0.04
Mortar with nano-Al_2O_3	29.32±6.60	385±79.4	0.69±0.09
Mortar with nano-TiO_2	35.66±4.66	345±12.6	0.59±0.04
Mortar with nano-SiO_2	206.5±2.9	128±46.5	0.86±0.08
Mortar with nano-Clay-hi	273.5±61.1	120±15.4	0.79±0.08
Mortar with nano-Clay-ho	487.9±69.6	113±22.9	0.91±0.39

Investigation by Field Emission Scanning Electron Microscopy

The FESEM test revealed that the admixing of nanomaterials not only led to denser cement mortar but also changed the morphology of cement hydration products. Figure 6*a* through 6*h* shows the FESEM images of mortar discs subsequent to the electromigration and electrochemical measurements. By examining the microstructure of the plain portland cement mortar disc (Figure 6*a* and 6*b*), it was found that cement hydration products existed mainly in the form of reticulated type II C-S-H gel, $Ca(OH)_2$ plate crystals, and needle-shaped crystals of calcium aluminum trisulfate hydrate (known as ettringite). Figure 6*c* though 6*f* shows the microstructure of mortar discs incorporating nano-Fe_2O_3, nano-Al_2O_3, nano-TiO_2, and nano-SiO_2, respectively. Distinguishing from the plain mortar, the nanomodified cement mortar was more dense and compact, especially when nano-SiO_2 was used. Figure 6*g* and 6*h* shows the microstructure of mortar discs incorporating the hydrophilic and hydrophobic nanomontmorillonite, respectively. The microstructure of the mortar modified by nanoclays not only contained more dense solid material but also featured high regularity due to the presence of sheet-like montmorillonite texture. In all the nanoparticles modified mortar specimens, reticulated type II C-S-H gel became dominant, whereas $Ca(OH)_2$ plate crystals and needle-shaped ettringite crystals were much less identifiable.

Role of Nanomaterials in Mortar Permeability and Microstructure

Building on existing research as well as the fresh evidence provided by this study, the mechanisms responsible for the effect of nanomaterials on mortar permeability and microstructure are proposed as follows.

First, all the nanomaterials may work as nanosized fillers and lead to a denser and less permeable microstructure of cement mortars. Transport of ionic and molecular species in concrete is mainly through pore solution. At the microscopic level, hydrated cement paste and ITZ are intrinsically microporous, both containing heterogeneous distributions of different types and amounts of solid phases, voids, and microcracks filled with air and pore solution. Pores larger than about 10 nm are related to the transport of species (*18*). As indirectly suggested by the electromigration, electrochemical, and FESEM results, the nanomaterials examined in this study might have modified the volume fraction, tortuosity, and connectivity of pores, all of which are critical to the transport properties of cement mortar (*19*).

Second, the nanomaterials may act as a "nucleus" to guide the formation and growth of cement hydration products. While only a small quantity of nanomaterials (1% by weight of cement) is used, their high SSA and high surface activity resulting from the nanosize effect may both promote the deposition of cement hydration products on them. As such, the hydration products were distributed more uniformly and better developed. This nucleus effect also inhibits the growth of $Ca(OH)_2$ and ettringite crystals and promotes the formation of reticulated type II C-S-H gel among hydrates. Cement paste consists of anhydrous clinker particles (1 to 50 μm), hydration products, and capillary pores (up to 1 μm in diameter). The hydration products usually consist mainly of C-S-H with a porosity of around 28% due to interlayer or gel pores (5 Å to 25 Å), and $Ca(OH)_2$ crystals (*19*). In addition, the needle-shaped ettringite crystals are formed during the early stages of hydration and eventually transform to hexagonal-plate crystals of monosulfate hydrate; calcium sulfoaluminates can also include other ingredients such as aluminoferrite to form Al_2O_3-Fe_2O_3-tri-x·SO_4 and Al_2O_3-Fe_2O_3-mono-x·SO_4 (*20*). The physicochemical properties of hydrated products are known to affect the transport characteristics of concrete. For instance, retarded transport of species due to physical trapping and chemical binding has been found closely related to the physicochemical properties of hydrated products in concrete matrix (*21*).

Third, the nanomaterials may promote the formation of high-density C-S-H structures via parallel packing. C-S-H is the main binding phase in portland cement–based materials (50% to 60% of the solids by volume) and its nature is central to the transport characteristics of concrete. Despite numerous publications, the exact structure of the C-S-H is still debatable, for its morphology varies from poorly crystalline fibers to reticular network. A quantitative "colloid" model proposed by Jennings' group provides probably the latest advances on the subject, describing the microstructure of C-S-H at the scale between 1 and 100 nm to rationalize many experimental observations (*22*). The basic building block of C-S-H was a unit simplified as a sphere approximately 2 nm across with an SSA of about 1,000 m^2/g. The units packed to form globules, which in turn packed together to form low-density and high-density C-S-H structures (*22*). An extended version of this model was formulated to account for new data obtained from small-angle neutron scattering, nanoindentation, and equilibrium drying measurements. It proposed that a loosely packed C-S-H formed initially as a random agglomeration of 5-nm C-S-H globules, which tended to densify to form low-density C-S-H structures via random jammed packing or to form high-density structures via parallel packing (*23*). The nanomaterials examined in this study likely facilitated the formation of high-density C-S-H structures, and the underlying mechanism for this effect remains a mystery to be explored.

Fourth, when nano-SiO_2 and nanomontmorillonites (containing high amount of SiO_2) are used, a pozzolanic reaction may occur between portland cement paste and the SiO_2 in nanomaterials. Such a reaction further inhibits the growth of $Ca(OH)_2$ and produces

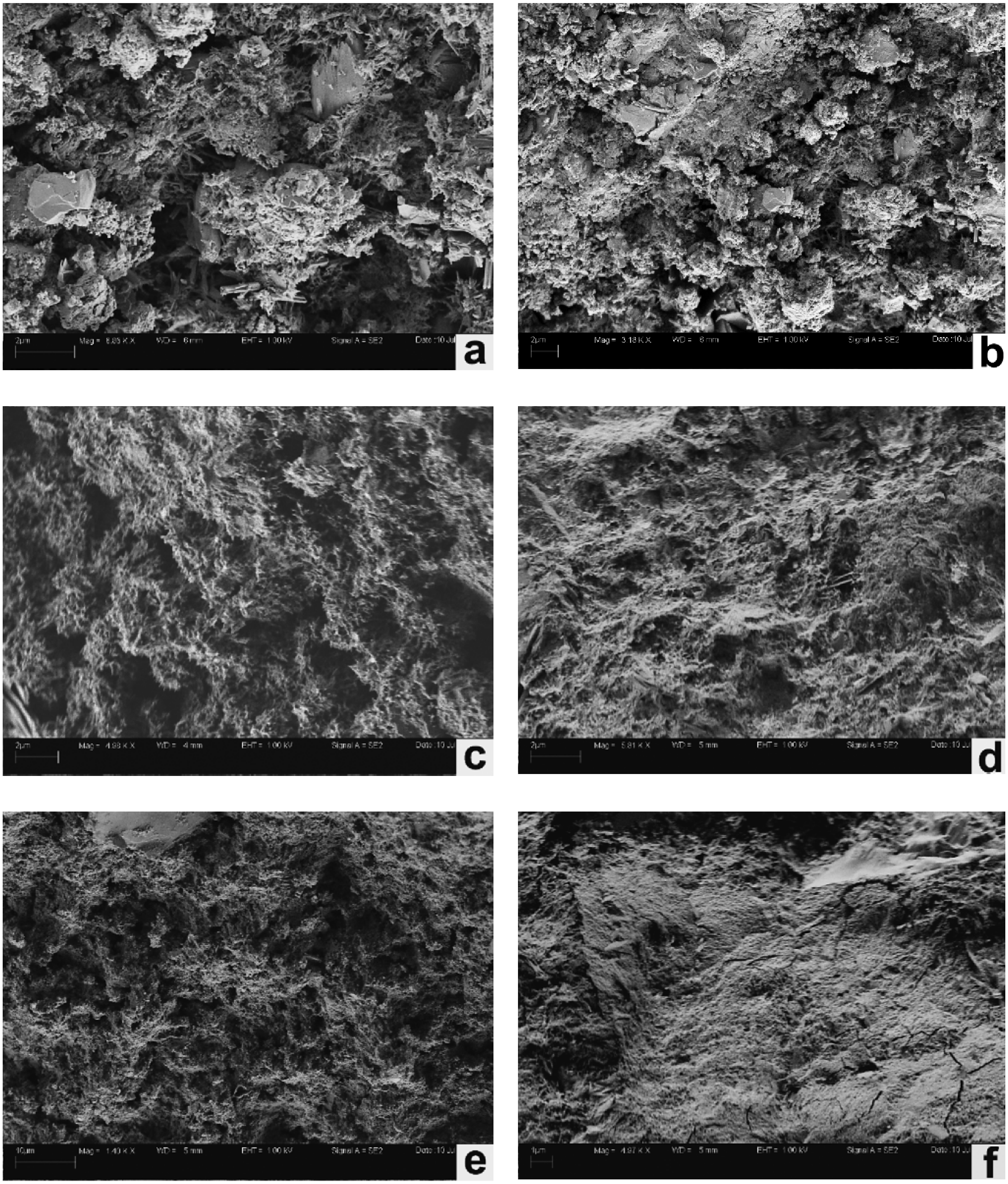

FIGURE 6 FESEM images of cement mortars: (*a*) and (*b*) without nanomaterial, (*c*) with nano-Fe_2O_3, (*d*) with nano-Al_2O_3, (*e*) with nano-TiO_2, (*f*) with nano-SiO_2. (Magnification for (*a*) to (*h*) at 6850, 3180, 4980, 5810, 1400, 4970, 1950, and 2840, respectively, to illustrate typical microstructure.)

(continued on next page)

FIGURE 6 *(continued)* **FESEM images of cement mortars: (*g*) with nano-Clay-hi, and (*h*) with nano-Clay-ho. (Magnification for (*a*) to (*h*) at 6850, 3180, 4980, 5810, 1400, 4970, 1950, and 2840, respectively, to illustrate typical microstructure.)**

reticulated type II C-S-H gel among hydrates. When nano-SiO_2 and nanomontmorillonites are used in concrete with large aggregates, this effect is expected to be magnified and lead to more improvements in the properties of concrete. In concrete, due to the high water-to-cement ratio at the large aggregate surface, the ITZ phase at aggregate–paste interface has a higher porosity than that of the paste phase and thus exerts a greater influence on the transport characteristics of concrete (*5*). Nano-SiO_2 and nanomontmorillonites are expected to tightly bond the cement hydration products within and around the transition zone, to reduce the $Ca(OH)_2$ crystal formed in the vicinity, and to form a dense and compact ITZ phase.

Finally, once nanomontmorillonites are mixed in fresh cement mixture, their nanosheets may be exfoliated in the cement matrix and tend to be dispersed in one direction under stirring. These nanosheets form ordered arrays due to their high aspect ratio and high surface activity. Such ordered arrays introduce microstructural regularity into cement mortars via a more stable bonding framework. They act as a dense barrier to reduce the permeability for ionic and molecular species as well as "fiber reinforcement" to enhance the mechanical properties of cement mortar. The nanomontmorillonites used in this study had a theoretical formula of $M_y^+(Al_{2-y}Mg_y)(Si_4)O_{10}(OH)_2 \cdot nH_2O$ and a high aspect ratio of 200 to 400 (approximately 1 nm thick and hundreds of nanometers in planar diameter). As shown in Figure 6*g* and 6*h*, the montmorillonite sheets were tightly embedded in the cement mortar featuring a texture of ordered array. The improvements in mortar properties and microstructure by the polysiloxane-modified montmorillonite were more significant than those by the unmodified nanomontmorillonite. This can be attributed to the hydrophobic nature as well as higher SAA of the polysiloxane-modified montmorillonite, which led to a denser and ordered microstructure of cement mortar, as shown in Figure 6*g* and 6*h*.

CONCLUSIONS

This paper presents an experimental study designed to examine the chloride permeability and microstructure of portland cement mortar with nanomaterials admixed at 1% by weight of cement.

The electromigration test showed that, for cement mortars of the same mix design, the incorporation of nanoparticles and nanoclays improved the chloride penetration resistance of the mortar, as indicated by the reduced apparent diffusion coefficients of chloride anion, D_{Cl^-}. When nano-SiO_2, hydrophilic nanomontmorillonite and hydrophobic nanomontmorillonite were admixed into fresh cement mortar at 1% by weight of cement, the value of D_{Cl^-} was decreased by 61.7%, 66.4%, and 76.0%, from 6.82×10^{-11} m^2/s (control specimen) to 2.61×10^{-11} m^2/s, 2.29×10^{-11} m^2/s, and 1.64×10^{-11} m^2/s, respectively. The nanomaterials also reduced the general ionic permeability of the mortar, as indicated by the reduced electric charge passing through, Q. As the SSA of nanomaterials increased, both D_{Cl^-} and Q decreased exponentially, indicating enhanced resistance to both the penetration of Cl^- and other ions into the mortar specimens. The electromigration test results revealed that the small amount of nano-SiO_2 and nanoclays markedly improved the chloride penetration resistance of the cement mortars.

The EIS test indicated that the incorporation of nanomaterials in cement mortar significantly increased its ionic transport resistance and decreased its electric capacitance, and again such effects were especially significant when using nano-SiO_2 and nanoclays.

The FESEM test revealed that the admixing of nanomaterials not only led to denser cement mortar but also changed the morphology of cement hydration products. In all the nanoparticles modified mortar specimens, reticulated type II C-S-H gel became dominant, whereas $Ca(OH)_2$ plate crystals and needle-shaped ettringite crystals were much less identifiable.

Mechanisms were proposed to explain the physicochemical changes induced by the nanomaterials and the SSA of nanomaterials was demonstrated to play a key role. First, all the nanomaterials may work as nanosized fillers and led to a denser and less permeable microstructure of cement mortars. Second, the nanomaterials may act as a nucleus to guide the formation and growth of cement hydration products. Third, the nanomaterials may promote the formation of high-density C-S-H structures via parallel packing. Fourth, when nano-SiO_2 and nanomontmorillonites are used, a pozzolanic reaction may occur between portland cement paste and the SiO_2 in nanomaterials. Finally, once nanomontmorillonites are mixed in fresh cement mixture, their nanosheets may be exfoliated in the cement matrix and tend to be dispersed in one direction under stirring. These nanosheets form ordered arrays due to their high aspect ratio and high surface activity. Such ordered arrays introduce microstructural regularity into cement mortars via a more stable bonding framework.

Considering the low cost of nanoclays, their use in concrete to reduce chloride permeability and to improve other properties of concrete is very promising. In the researchers' laboratory, work is planned to further investigate the potential synergy between nanomontmorillonites and other admixtures in improving the durability of cement-based composite materials.

ACKNOWLEDGMENTS

This work was supported by the Research and Innovative Technology Administration under the U.S. Department of Transportation through the University Transportation Center research grant.

REFERENCES

1. A Critical Investor's Guide to Nanotechnology, Feb. 2002. www.inrealis.com/nano. Accessed Jan. 20, 2007.
2. Jensen, O. M., and P. F. Hansen. Water-Entrained Cement-Based Materials: I. Principles and Theoretical Background. *Cement and Concrete Research,* Vol. 31, 2001, pp. 647–654.
3. Basheer, L., J. Kropp, and D. J. Cleland. Assessment of the Durability of Concrete from Its Permeation Properties. *Construction and Building Materials,* Vol. 15, No. 2, 2001, pp. 93–113.
4. Baykal, M. *Implementation of Durability Models for Portland Cement Concrete into Performance-Based Specifications.* University of Texas at Austin, Austin, 2000.
5. Savas, B. Z. *Effects of Microstructure on Durability of Concrete.* PhD thesis. North Carolina State University, Raleigh, 2000.
6. Mehta, P. L., and D. Manmohan. Pore Size Distribution and Permeability of Hardened Cement Pastes. *Proc., 7th International Congress on the Chemistry of Cements,* Vol. III, Editions Septima, Paris, 1980, pp. 1–5.
7. Maso, J. C. The Bond Between Aggregates and Hydrated Cement Pastes. *Proc., 7th International Congress on the Chemistry of Cements,* Vol. I, Editions Septima, Paris, 1980, pp. 3–15.
8. Li, H., H.-G. Xiao, J. Yuan, and J. Ou. Microstructure of Cement Mortar with Nano-Particles. *Composites Part B: Engineering,* Vol. 35, No. 2, 2004, pp. 185–189.
9. Ji, T. Preliminary Study on the Water Permeability and Microstructure of Concrete Incorporating Nano-SiO_2. *Cement and Concrete Research,* Vol. 35, 2005, pp. 1943–1947.
10. Tsai, C.-F. *A Study of the Effect of Nanomaterials on Properties of Concrete* (in Chinese). Master's thesis, Chung Yuan Christian University, Taiwan, Republic of China, 2005. thesis.lib.cycu.edu.tw/ETD-db/ETD-search/view_etd?URN=etd-0724105-170157. Accessed July 25, 2007.
11. Birgisson, B. Nanomodification of Cement Paste to Improve Bulk Properties of Concrete. *National Science Foundation Workshop on Nanomodification of Cementitious Materials,* University of Florida, Aug. 2006. www.ce.ufl.edu/nanoworkshop/Birgisson.pdf. Accessed July 27, 2007.
12. Chang, T.-P., J.-Y. Shih, J.-M. Yang, and T.-C. Hsiao. Material Properties of Portland Cement Paste with Nano-Montmorillonite. *Journal of Materials Science,* Vol. 42, No. 17, 2007, pp. 7478–7487.
13. Lomborg, B. *The Skeptical Environmentalist: Measuring the Real State of the World.* Cambridge University Press, Cambridge, United Kingdom, 2001, pp. 512–540.
14. Hausmann, D. A. A Probability Model of Steel Corrosion in Concrete. *Materials Performance,* Vol. 37, No. 10, 1998, pp. 64–68.
15. Hartt, W., S. Charvin, and S. Lee. Influence of Permeability Reducing and Corrosion Inhibiting Admixtures in Concrete upon Initiation of Salt Induced Embedded Metal Corrosion. Final Report, 1999. www.dot.state.fl.us/research-center/Completed_Proj/Summary_SMO/FDOT_0510716_rpta.pdf. Accessed July 1, 2008.
16. Wee, T. H., A. K. Suryavanshi, and S. S. Tin. Evaluation of Rapid Chloride Permeability Test (RCPT) Results for Concrete Containing Mineral Admixtures. *ACI Materials Journal,* Vol. 97, No. 2, 2000, pp. 221–232.
17. Atkins, P. W. *Physical Chemistry,* 5th ed. Oxford University Press, Oxford, United Kingdom, 1994.
18. Russel, W. B., D. A. Saville, and W. R. Schowalter. *Colloidal Dispersions.* Cambridge University Press, Cambridge, United Kingdom, 1989.
19. Buenfeld, N. R., G. K. Glass, A. M. Hassanein, and J. Z. Zhang. Chloride Transport in Concrete Subjected to Electric Field. *Journal of Materials in Civil Engineering,* Vol. 10, No. 4, 1998, pp. 220–228.
20. Richardson, I. G. The Nature of the Hydration Products in Hardened Cement Pastes. *Cement and Concrete Composites,* Vol. 22, 2000, pp. 97–113.
21. Xi, Y., and Z. Bazant. Modeling Chloride Penetration in Saturated Concrete. *Journal of Materials in Civil Engineering,* Vol. 11, No. 1, 1999, pp. 58–65.
22. Jennings, H. M. A Model for the Microstructure of Calcium Silicate Hydrate in Cement Paste. *Cement and Concrete Research,* Vol. 30, No. 1, 2000, pp. 101–116.
23. Tennis, P. D., and H. M. Jennings. A Model for Two Types of C-S-H in the Microstructure of Portland Cement Pastes. *Cement and Concrete Research,* Vol. 30, No. 6, 2000, pp. 855–863.

The Nanotechnology-Based Concrete Materials Task Force sponsored publication of this paper.